

Enhanced Efficiency and Dynamic Performance in Wind Power Generation Systems using Artificial Neural Networks and Predictive Current Control for PMSG-based Turbines

Benameur Afif¹ , Mohamed Salmi² , Mohammed Berka³ ,
Riyadh Ramadhan kreedeegh⁴ , Muhammad Tahir⁵ .

^{1,3}Department of Electrotechnic, University Mustapha Stambouli of Mascara, Mascara 29000, Algeria.

²Department of Physics, University of M'sila, M'sila 28000, Algeria

^{4,5}Chemical and Petroleum Engineering Department, UAE University, Al Ain, United Arab Emirates.

⁴Department of Analysis and Quality Control, Sarir Oil Refinery, Arabian Gulf Oil Company, El Kish, Benghazi, Libya.

⁴Libyan Advanced Center for Chemical Analysis, Libyan Authority for Scientific Research, Tripoli, Libya.

E-mail: ¹ b.afif@univ-mascara.dz, ² mohamed.salmi@univ-msila.dz, ³ m.barka@univ-mascara.dz,
⁴ riyadhkridiegh@gmail.com, ⁵ muhammad.tahir@uaeu.ac.ae.

ARTICLE INFO.

Article history:

Received 21 Dec 2024

Received in revised form 23 Dec 2024

Accepted 21 Feb 2025

Available online 28 Feb 2025

KEYWORDS

Predictive Current Control (PCC); Artificial Neural Networks (ANN); Wind Energy Conversion System (WECS); Maximum Power Point Tracking (MPPT); Permanent Magnet Synchronous Generator (PMSG); Grid Integration.

ABSTRACT

Recently, wind power generation systems have seen significant developments aimed at improving performance and efficiency. Permanent magnet synchronous generators (PMSG) are essential for wind power production systems because of their exceptional power density, high efficiency, and dependable operation. These properties enable PMSGs to effectively convert wind energy into electrical energy with minimal losses and high accuracy. This study proposes an enhanced control system for wind power generation using permanent magnet synchronous generators (PMSG), integrating artificial neural networks (ANN) and predictive current control (PCC) techniques to optimize efficiency and dynamic performance.

Traditional control systems often require wind speed measurement and utilize separate loops for speed and current regulation. In contrast, the proposed approach eliminates the need for wind speed sensing by employing an ANN to estimate optimal reference currents based solely on rotational speed measurements. PCC is then applied to regulate the generator currents, replacing conventional PI controllers. This configuration enables the removal of the speed regulation loop while maintaining maximum power point tracking capability.

*Corresponding author.



Simulation results demonstrate that the ANN-PCC control system achieves superior dynamic response and higher overall efficiency compared to conventional methods. The system exhibits faster tracking of maximum power points, reduced total harmonic distortion, and enhanced stability under variable wind conditions. Additionally, the proposed controller simplifies the overall system architecture by reducing sensor requirements and control loops. The paper presents a comprehensive comparison between the proposed ANN-PCC system and two conventional control methods: a perturbation and observation (P&O) algorithm with PI control, and a tip speed ratio (TSR) technique with PI control. Results show that the ANN-PCC approach outperforms both conventional methods in terms of response time, power output stability, and grid current quality. These improvements make the ANN-PCC approach a promising solution for increasing the performance and reliability of PMSG-based wind energy conversion systems in grid-connected applications, potentially contributing to the broader adoption of wind power technology.

تحسين الفعالية والأداء الديناميكي في أنظمة توليد طاقة الرياح باستخدام الشبكات العصبية الاصطناعية والتحكم التنبؤي بالتيار للتوربينات القائمة على المولدات المتزامنة ذات المغناطيسية الدائمة

بن عامر عفيف، محمد سالي، محمد بركتة، رياض رمضان كريدغ، محمد طاهر.

ملخص: في الآونة الأخيرة، شهدت أنظمة توليد طاقة الرياح تطورات كبيرة تهدف إلى تحسين الأداء والكفاءة. تعد المولدات المتزامنة ذات المغناطيس الدائم ضرورية لأنظمة إنتاج طاقة الرياح بسبب كثافتها الاستثنائية في الطاقة وكفاءتها العالية وتشغيلها الموثوق. تمكن هذه الخصائص مولدات الطاقة الشمسية PMSG من تحويل طاقة الرياح إلى طاقة كهربائية بشكل فعال مع الحد الأدنى من الخسائر والدقة العالية. تقترح هذه الدراسة نظام تحكم معزز لتوليد طاقة الرياح باستخدام مولدات متزامنة ذات مغناطيس دائم (PMSG)، ودمج الشبكات العصبية الاصطناعية (ANN) وتقنيات التحكم في التيار التنبؤي (PCC) لتحسين الكفاءة والأداء الديناميكي. تتطلب أنظمة التحكم التقليدية غالباً قياس سرعة الرياح واستخدام حلقات منفصلة لتنظيم السرعة والتيار. وعلى النقيض من ذلك، يلغي النهج المقترح الحاجة إلى استشعار سرعة الرياح من خلال استخدام شبكة عصبية اصطناعية لتقدير التيارات المرجعية المثلى بناءً على قياسات سرعة الدوران فقط. بعد ذلك يتم تطبيق PCC لتنظيم تيارات المولد، واستبدال وحدات التحكم PI التقليدية. يتيح هذا التكوين إزالة حلقة تنظيم السرعة مع الحفاظ على قدرة تتبع نقطة الطاقة القصوى. توضح نتائج المحاكاة أن نظام التحكم ANN-PCC يحقق استجابة ديناميكية متفوقة وكفاءة إجمالية أعلى مقارنة بالطرق التقليدية. يُظهر النظام تتبعاً أسرع لنقاط الطاقة القصوى، وتشوهات توافقية إجمالية أقل، واستقراراً معززاً في ظل ظروف الرياح المتغيرة. بالإضافة إلى ذلك، يعمل المتحكم المقترح على تبسيط بنية النظام الإجمالية عن طريق تقليل متطلبات المستشعر وحلقات التحكم. تقدم الورقة مقارنة شاملة بين نظام ANN-PCC المقترح وطريقتي تحكم تقليديتين: خوارزمية الاضطراب والملاحظة (P&O) مع التحكم PI، وتقنية نسبة سرعة الطرف (TSR) مع التحكم PI. تظهر النتائج أن نهج ANN-PCC يتفوق على كل من الطرق التقليدية من حيث وقت الاستجابة، استقرار مخرجات الطاقة وجودة تيار الشبكة. تجعل هذه التحسينات نهج ANN-PCC حلاً واعداً لزيادة أداء وموثوقية أنظمة تحويل طاقة الرياح القائمة على PMSG في التطبيقات المتصلة بالشبكة، مما قد يساهم في تبني تكنولوجيا طاقة الرياح على نطاق أوسع.

الكلمات المفتاحية – التحكم في التيار التنبؤي، الشبكات العصبية الاصطناعية، نظام تحويل طاقة الرياح، تتبع نقطة الطاقة القصوى، مولد متزامن ذو مغناطيس دائم، تكامل الشبكة.

1. INTRODUCTION

By the 2050s, projections indicate a staggering global population of 9 billion, driving an unprecedented surge in energy demand fueled by our increasing reliance on electronic devices and the continuous growth of industries. This demographic shift presents significant challenges to our current energy paradigm, which heavily relies on traditional fossil fuels. These conventional energy sources are proving increasingly unsustainable due to their finite nature, price volatility, and devastating environmental impact. The limitations of fossil fuels are becoming more apparent, necessitating a shift towards more sustainable alternatives. In light of these challenges, Renewable Energy Sources (RESs) have emerged as a promising solution to meet our future energy needs. RESs, particularly wind and solar power, offer sustainable and clean energy production without harmful emissions. Moreover, technological advancements and economies of scale have significantly improved the cost-competitiveness of RESs, making them increasingly viable and attractive options for future power generation. Global efforts are now heavily focused on developing and refining wind energy technologies, although other RESs such as solar and geothermal energy also hold immense potential. As we look towards the long term, RESs are undeniably key to meeting our growing energy demands while minimizing environmental impact. The transition to renewable energy sources is not just a technological challenge but also a societal imperative [1-4]. By embracing these renewable resources, we have the opportunity to create a more sustainable and environmentally friendly future for generations to come. This shift towards RESs represents a crucial step in addressing climate change, reducing our carbon footprint, and ensuring energy security in an increasingly resource-constrained world. The development and widespread adoption of RESs will play a pivotal role in shaping a more sustainable and resilient global energy landscape.

Wind energy has captured significant attention from researchers and industry experts due to its inherent advantages: clean energy generation, rapid technological development, and increasing cost-competitiveness with traditional electricity sources. The surge in installed wind energy conversion system (WECS) capacity has driven extensive exploration and validation of various WECS designs. These systems can be broadly categorized into two main types: fixed-speed and variable-speed. While fixed-speed WECS offer simplicity and lower upfront costs, variable-speed systems have emerged as the preferred choice due to their superior efficiency. This advantage stems from their ability to adjust generator speed dynamically, allowing them to operate at the maximum power point for optimal energy extraction from available wind resources [5-7]. The flexibility of variable-speed systems enables them to adapt to changing wind conditions, maximizing energy yield across a wide range of wind speeds. Furthermore, variable-speed WECS often incorporate advanced control strategies and power electronics, enhancing their grid integration capabilities and overall system performance. As wind energy technology continues to evolve, the focus on optimizing variable-speed WECS remains a key area of research and development in the renewable energy sector.

Among renewable energy technologies, variable-speed wind energy generating systems (VS-WEGs) are experiencing rapid growth, offering numerous advantages that make them a competitive choice for sustainable green energy production. VS-WEGs achieve high efficiency primarily through the use of permanent magnet synchronous generators (PMSGs), which boast high power density and ease of implementation. These systems reduce the need for complex mechanical components, contributing to increased overall reliability and reduced maintenance costs. The flexible operation of VS-WEGs allows for better wind energy utilization and improved annual energy production across diverse wind conditions. Moreover, VS-WEGs produce zero harmful emissions, supporting environmental protection efforts and mitigating climate change. PMSGs offer superior performance at low wind speeds, making them highly suitable for a wide

range of wind energy projects in various geographical locations. This characteristic extends the viability of wind power to areas previously considered unsuitable. However, VS-WECS faces challenges such as wind speed variability, necessitating sophisticated control systems to ensure operational stability and efficiency [8-10]. These control systems must adapt rapidly to changing wind conditions, optimize power output, and maintain grid stability. As research continues, addressing these challenges through advanced control algorithms and system designs remains a key focus in maximizing the potential of VS-WECS technology.

Despite their promise, RES like solar and wind power face a challenge: their output fluctuates significantly. This variability is directly tied to weather patterns, with factors like solar radiation and temperature impacting solar panels, and wind speed affecting wind turbines. To address this issue and ensure these systems operate efficiently, MPPT algorithms are employed. MPPT ensures the wind turbine operates at its peak performance, adapting to fluctuating wind speeds and contributing to grid stability by providing consistent power output. Overall, MPPT plays a vital role in maximizing wind energy system performance, sustainability, and economic viability [11-14]. Leveraging vector control (VC), the proposed control strategy in [15] tackles multiple objectives in the PMSG wind turbine system: maximizing power capture through MPPT based on the tip speed ratio (TSR) technique, maintaining constant DC link voltage, and controlling both generator and grid side converters. This matter grants control over the reactive power injected into the network. The control algorithm in [16] leverages a linear disturbance observer (DOB) to estimate wind turbine aerodynamic torque. This estimate is then used in a feed-forward compensation scheme and combined with a numerical zero search of a nonlinear function to determine the wind speed, ultimately setting the reference PMSG speed based on the TSR technique. In [17], a comparison between an adaptive fuzzy logic control system and a proportional-integral (PI) control system was presented to regulate the PMSG speed. The reference speed was terminated based on the TSR technique. A PI controller was used to regulate the currents in the inner loop and control the DC voltage and currents for GSC. Work in Ref. [18] presents the dynamic model, parameter measurement, and control of a variable speed WECS system using PMSG. The primary PMSG parameters may be monitored experimentally, and the measured values are utilized for controller design. The VC system optimizes power extraction under varying wind speeds by controlling the generator's side converter based on the TSR technique. By regulating the d and q-axis currents, an MPC of a grid-side converter (GSC) can govern the flows of both active and reactive electricity to the grid. The authors of [19] used the active disturbance rejection control strategy to effectively regulate the WECS, achieving MPPT based on the OTC technique, maintaining DC-link voltage stability, and good regulation of reactive power. Work in Ref. [20] provides a comparison between optimal torque control (OTC) and TSR MPPT techniques. A fuzzy logic controller (FLC) is proposed as an alternative to the PI controller to achieve performance compatible with the current control loop of MSC. Regarding tracking the maximum power point, the results showed that TSR excels with its rapid response to wind speed changes, but suffers from delivering less smooth output power. In contrast, OTC prioritizes smooth output power, sacrificing responsiveness to wind speed fluctuations. The strategy in [21] leverages a fuzzy fractional order proportional-integral (FFOPI) controller for the machine side converter (MSC). This approach aims to determine the reference value of current on the q-axis to achieve max power under varying wind speeds like the OTC technique. A PI controller was used in the inner loop to regulate the currents. Moreover, in work in [22], a cascade neural network (CNN)-based MPPT algorithm was used to extract maximum power in a wind generation system including PMSG, diode rectifier, dc-dc Bi-directional converter and storage system (battery). Simulated and experimental data were used, respectively, to train and test the CNN. The performance of the CNN-based MPPT was also contrasted with that of the

feed-forward MPPT system. The proposed method shows maximum power extraction with a simple design and more flexibility to vary wind speed.

Because of all these motivations, this study presents a comprehensive approach to enhancing the efficiency and dynamic performance of wind power generation systems using Permanent Magnet Synchronous Generators (PMSG). Our method integrates advanced control techniques, specifically Artificial Neural Networks (ANN) and Predictive Current Control (PCC), to optimize system performance. The work plan is structured in several key phases. Initially, we developed a detailed model of the wind turbine system, including the aerodynamic, mechanical, and electrical components. This model serves as the foundation for subsequent control system design and simulation. Next, we implement and evaluate three distinct control strategies: a conventional Perturbation and Observation (P&O) algorithm with PI control, a Tip Speed Ratio (TSR) technique with PI control, and our proposed ANN-PCC approach. The ANN is trained using data from optimal operating points to estimate reference currents based on rotational speed, eliminating the need for wind speed measurement. Concurrently, we design the PCC algorithm to regulate generator currents, replacing traditional PI controllers. We then conduct extensive simulations to compare the performance of these three control strategies under various wind conditions. Our analysis focuses on key performance indicators such as maximum power point tracking efficiency, dynamic response time, power output stability, and grid current quality. Additionally, we evaluate the system's behavior during wind speed fluctuations and assess the overall energy yield. The final phase of our work involves a critical analysis of the simulation results, highlighting the advantages and potential limitations of the proposed ANN-PCC system. We also discuss the implications of our findings for the broader field of wind energy conversion systems and suggest areas for future research and development.

The novelties and advantages of this work lie in the following points.

1. Integration of Artificial Neural Networks (ANN) with Predictive Current Control (PCC): This novel combination allows for efficient maximum power point tracking without the need for wind speed measurement, simplifying the system architecture.
2. Elimination of the speed regulation loop: The proposed system removes the need for a separate speed control loop, reducing system complexity while maintaining high performance.
3. Improved dynamic response: The ANN-PCC system demonstrates faster tracking of maximum power points compared to conventional control methods, enhancing overall system efficiency.
4. Reduced current Total Harmonic Distortion (THD): The proposed control strategy results in lower THD in grid currents, improving power quality and grid integration.
5. Enhanced stability under variable wind conditions: The system shows better performance and stability during wind speed fluctuations, increasing the reliability of wind power generation.
6. Simplified sensor requirements: By eliminating the need for wind speed measurement, the system reduces hardware complexity and potential points of failure, potentially improving long-term reliability and reducing maintenance costs.

The remainder of this paper is organized as follows: Section 2 presents a comprehensive system modeling, detailing the wind turbine aerodynamics, PMSG dynamics, and grid-side converter. Section 3 delves into the control systems, describing the conventional PI control for the grid-side converter, as well as the PI and PCC approaches for PMSG control. It also elaborates on the proposed ANN-based MPPT system. Section 4 presents the simulation results, providing a comparative analysis of the proposed ANN-PCC system against conventional P&O-PI and TSR-PI control methods. This section showcases the system's performance under varying wind conditions, highlighting improvements in speed response, current regulation, power tracking, and grid current quality. Section 5 concludes the paper, by summarizing the key findings and

discussing the implications of the proposed control strategy for wind energy conversion systems. Additionally, it suggests potential directions for future research in this field.

2. SYSTEM MODELLING

In this section, we give an outline of the system for converting wind energy. Figure 1 shows the architecture of the system, which is mostly based on a PMSG and uses three main subsystems which are:

- Aerodynamic system: convert wind energy into a mechanical one.
- PMSG system: This system converts mechanical energy from the aerodynamic system into electrical energy.
- Electrical power transmission system: It consists of a two-stage electronic converter (back-to-back) controlled based on VC theory to regulate the power flow to and from the electrical network.

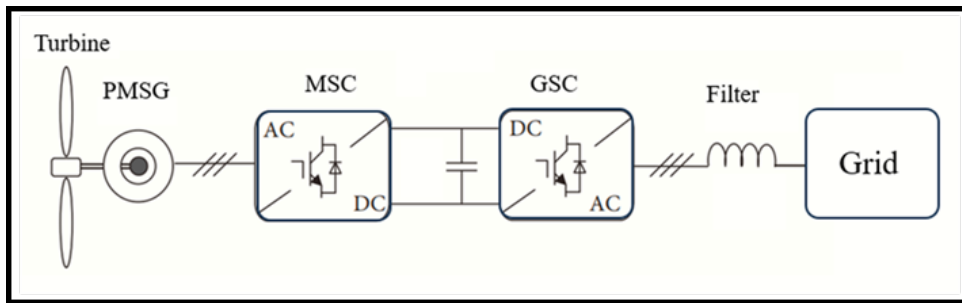


Figure 1. The structure of WECS based on PMSG.

2.1. Wind turbine model

The kinetic energy of wind is estimated through the following expression.

$$P_{wind} = 0.5\rho\pi R^2V^3 \quad (1)$$

Here, ρ denotes air density, R represents the length of the turbine blade, and V denotes wind speed. Eq (2) determines how much mechanical power the turbine can extract from the wind's motion.

$$P_t = P_{wind} C_p(\beta, \lambda) \quad (2)$$

Where: C_p is a Power coefficient, β is the pitch angle, and λ is the TSR. The power coefficient can be defined as [1, 3].

$$C_p = 0.5 \left(116 \left(\frac{1}{\lambda + 0.08\beta} - \frac{0.035}{\beta^3 + 1} \right) - 0.4\beta - 5 \right) e^{-21 \left(\frac{1}{\lambda + 0.08\beta} - \frac{0.035}{\beta^3 + 1} \right)} + 0.0068\lambda \quad (3)$$

Figure 2 presents the power coefficient (C_p) characteristics of the wind turbine as a function of the tip speed ratio (λ) and pitch angle (β). The graph demonstrates the relationship between these parameters, which is crucial for understanding the turbine's performance under various operating conditions. Notably, the figure shows that the power coefficient reaches its maximum value when λ is approximately 8.2. This optimal point is significant for the design of maximum power point tracking (MPPT) algorithms, as it represents the condition where the turbine extracts the most energy from the wind. The multiple curves for different pitch angles illustrate how adjusting the blade pitch can affect the power coefficient, providing insight into turbine control strategies for different wind speeds.

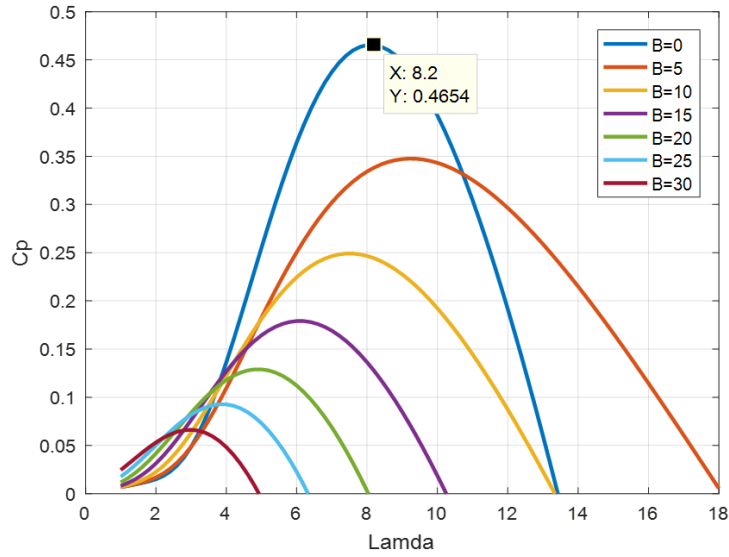


Figure 2. Power coefficient characteristics.

Equation (4) gives the TSR as follows.

$$\lambda = \frac{R\omega_m}{V} \quad (4)$$

Where ω_m denotes the mechanical speed of the turbine. The aerodynamic torque can be computed using the subsequent equation.

$$T_{mech} = \frac{P}{\omega_m} \quad (5)$$

2.2. A Dynamic model for PMSG in the d-q coordinates

The PMSG has a three-phase winding system with a 120° phase shift between each of the windings in its stator. Permanent magnets are used to excite the rotor. Using the conventional simplifying in the d-q frame, the PMSG is modeled. Equations (6) and (7) describe the mathematical formulation of the PMSG in the Park reference frame and equation (8) describes the mechanical formulation for surface-mounted PMSG [4, 5].

$$L_{mq} \frac{di_{md}}{dt} - \omega L_{md} i_{mq} + R_{ms} i_{md} = V_{md} \quad (6)$$

$$L_{mq} \frac{di_{mq}}{dt} + \omega L_{md} i_{md} + \omega \Phi_m + R_{ms} i_{mq} = V_{mq} \quad (7)$$

$$\frac{d\omega_m}{dt} = \frac{1.5p\Phi_m i_{mq}}{J} - \frac{T_{mech}}{J} - \frac{f}{J} \omega_m \quad (8)$$

Where V_{md} , V_{mq} , are *d*-axis and *q*-axis PMSG voltages. i_{md} , i_{mq} are *d*-axis and *q*-axis PMSG currents. L_{md} , L_{mq} are inductances of stator coils in *d-q* frame. Φ_m Magnet flux, R_{ms} represents the stator resistance. J denotes inertia. f is the frictional constant. ω is the electrical speed, which is given according to the following relation.

$$\omega = p\omega_m \quad (9)$$

Here p represents the pole pair.

2.3. Grid-side converter modeling

GSC permits current flow from and to the grid, which means converting DC voltage to AC

voltage, or vice versa [23, 24].

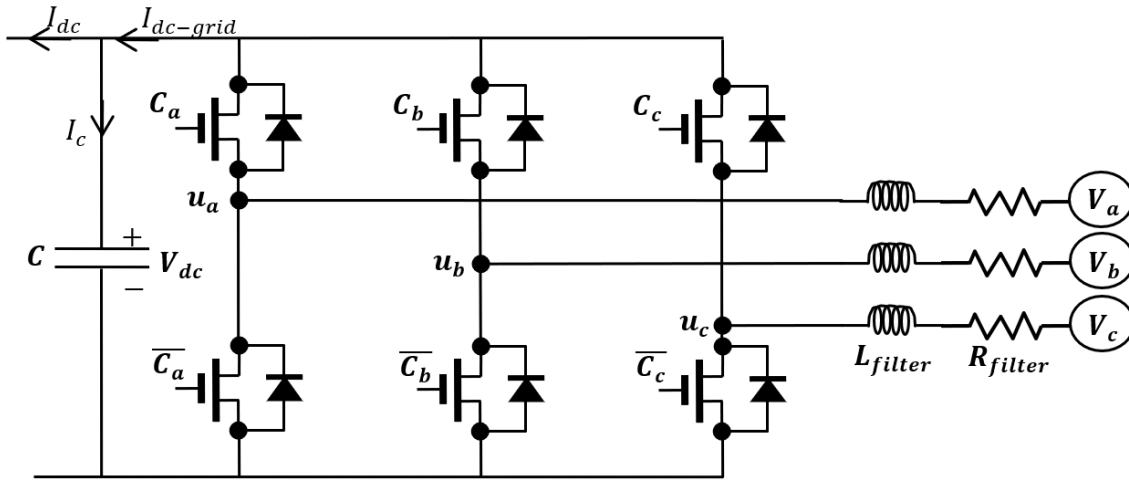


Figure 3. The grid-side converter.

Where (C_a, C_b, C_c) , (u_a, u_b, u_c) , and (V_a, V_b, V_c) represent pulses applied on transistors, voltages in the GSC columns and grid voltages, respectively.

Figure 3 illustrates the structure of the grid-side converter (GSC) in the wind energy conversion system. The GSC plays a crucial role in interfacing the DC link with the three-phase AC grid. It consists of six switches arranged in three columns, each connected to the grid through identical coils with L_{filter} inductance and R_{filter} resistance. The figure clearly shows the relationship between the control pulses (C_a, C_b, C_c) applied to the transistors, the resulting voltages in the GSC columns (u_a, u_b, u_c) , and the grid voltages (V_a, V_b, V_c) . This configuration allows for bidirectional power flow, enabling the system to convert DC voltage to AC voltage or vice versa, which is essential for efficient grid integration of the wind energy system. The following is how a GSC can be expressed in a d-q frame [23, 24].

$$V_d = R_{filter} i_d + L_{filter} \frac{di_d}{dt} - \omega_s L_{filter} i_q + u_d \tag{10}$$

$$V_q = R_{filter} i_q + L_{rec} \frac{di_q}{dt} + \omega_s L_{filter} i_d + u_q \tag{11}$$

$$C \frac{dV_{dc}}{dt} = i_{dc-grid} - i_{dc} \tag{12}$$

Where V_d, V_q , are d - and q -axis grid voltages, i_d, i_q are the d and q -axis grid, C is the DC link capacitor. u_d, u_q are the d - and q -axis converter voltages. The voltages in the GSC columns depend on the DC link voltage (V_{dc}) and pulses applied on transistors as [23].

$$\begin{bmatrix} u_a \\ u_b \\ u_c \end{bmatrix} = \frac{V_{dc}}{3} \begin{bmatrix} 2 & -1 & -1 \\ -1 & 2 & -1 \\ -1 & -1 & 2 \end{bmatrix} \begin{bmatrix} C_a \\ C_b \\ C_c \end{bmatrix} \tag{13}$$

3. CONTROL SYSTEMS

3.1. GSC control system

Figure 4 illustrates the schematic of the Grid Side Converter (GSC) PI control system. This control system aims to regulate the DC link voltage and control the currents flowing to and from the grid. It employs a cascaded control structure with an outer loop for DC voltage regulation and an inner loop for current control. The outer loop generates the reference for the d -axis current (i_{d-ref}) based on the difference between the desired and actual DC link voltage. The inner current control loop regulates both d -axis and q -axis currents. By setting the q -axis current reference (i_{q-ref}) to zero, the system achieves unity power factor operation. The control outputs are then transformed back to the (a,b,c) frame to generate the appropriate switching signals for the GSC. The electrical power passed by the GSC is expressed by [7, 8].

$$P = 1.5V_d i_d \tag{14}$$

$$Q = -1.5V_d i_q \tag{15}$$

Thus, the current i_q is set to zero to achieve a unit power factor.

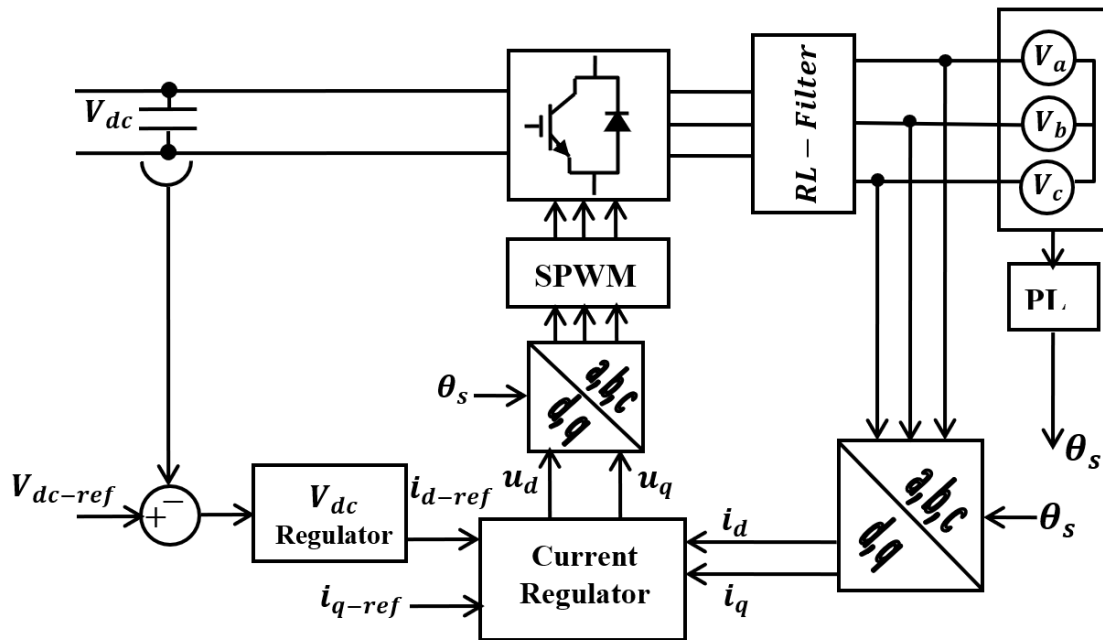


Figure 4. Schematic of GSCPI control system.

3.2. MSC control system

3.2.1. PI control of PMSG speed and currents

Figure 5 presents the structure of the PI control system for the speed and currents of the Permanent Magnet Synchronous Generator (PMSG). This control scheme employs a dual-loop configuration. The outer loop is responsible for regulating the generator's speed, comparing the actual speed to the reference value provided by the Maximum Power Point Tracking (MPPT) unit. The speed controller generates the reference value for the q -axis current. For a surface-mounted PMSG, the control system aims to maintain the d -axis stator current at zero. The inner loop focuses on current regulation, controlling both d -axis and q -axis currents. This nested control structure allows for precise management of the generator's speed and torque, which is crucial for optimal power extraction from the wind turbine. The control outputs are then transformed from

the d-q [9] reference frame back to the (a,b,c) frame to generate the appropriate switching signals for the Machine Side Converter (MSC). This control strategy enables efficient operation of the PMSG under varying wind conditions.

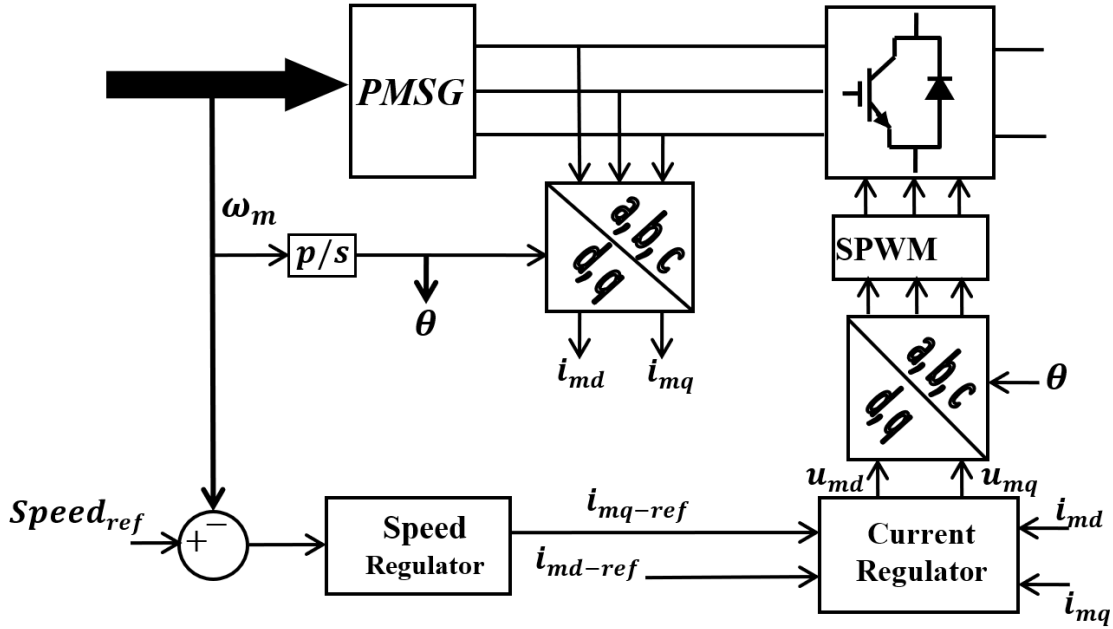


Figure 5. Schematic of PMSG PI control system.

3.2.2. PCC of PMSG currents

The research community has recently turned its attention to MPC because of the advancement of high-computational processors. This is because MPC can handle nonlinearities, multivariable, and system constraints in an advanced automatic manner with ease [25-26]. Using an MSC, a predictable amount of switching potential vectors is generated with the use of predictive current control (PCC). To do this, currents at the MSC terminal are predicted for each switching vector the MSC produces using a PMSG model. The proper switching vector can thus be selected using an objective function that is defined. This objective function goal is to reduce the discrepancy between the stator's anticipated current and reference currents. To control the MSC, the switching vector that yields the lowest value of the goal function is chosen. There is no need for a modulation stage or linear regulator with this controller.

The vector difference between the stator's anticipated current $\vec{I}_p(k+1)$ and reference currents $\vec{I}_{ref}(k+1)$ is calculated by the following objective function.

$$\vec{g} = \vec{I}_{ref}(k+1) - \vec{I}_p(k+1) \quad (16)$$

Where, $\vec{I}_{ref}(k+1) = I_{\alpha-ref}(k+1) + jI_{\beta-ref}(k+1)$, $\vec{I}_p(k+1) = I_{\alpha-p}(k+1) + jI_{\beta-p}(k+1)$.

In addition, $I_{\alpha-ref}(k+1)$, $I_{\alpha-p}(k+1)$ and $I_{\beta-ref}(k+1)$, $I_{\beta-p}(k+1)$ are the direct and quadrature components of the current vector $\vec{I}_{ref}(k+1)$ and $\vec{I}_p(k+1)$, respectively in α, β frame.

Figure 6 illustrates the structure of the Predictive Current Control (PCC) system for the Permanent Magnet Synchronous Generator (PMSG). This advanced control technique operates on a discrete model of the PMSG. The process begins with measuring the voltage at the Machine Side Converter (MSC) terminals and the stator currents. The system then estimates the back electromotive force and predicts the future current values $\vec{I}_p(k+1)$ based on potential voltage

vectors. A cost function is employed to evaluate these predictions against the reference currents. The voltage vector that minimizes this cost function is selected for implementation. This approach eliminates the need for a modulation stage or linear regulator, potentially offering faster dynamic response and more precise current control compared to traditional PI-based systems. The PCC algorithm repeats this process at each sampling interval (T_s), continuously optimizing the PMSG's current control. This method can potentially improve the overall efficiency and performance of the wind energy conversion system.

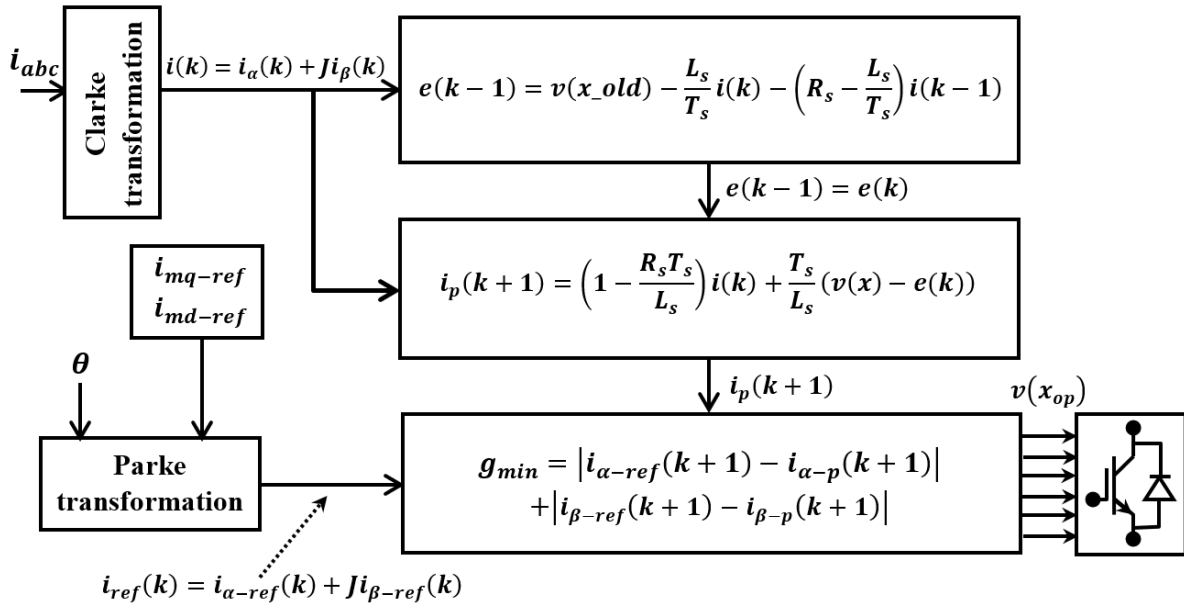


Figure 6. The structure of the PMSG currents predictive control system.

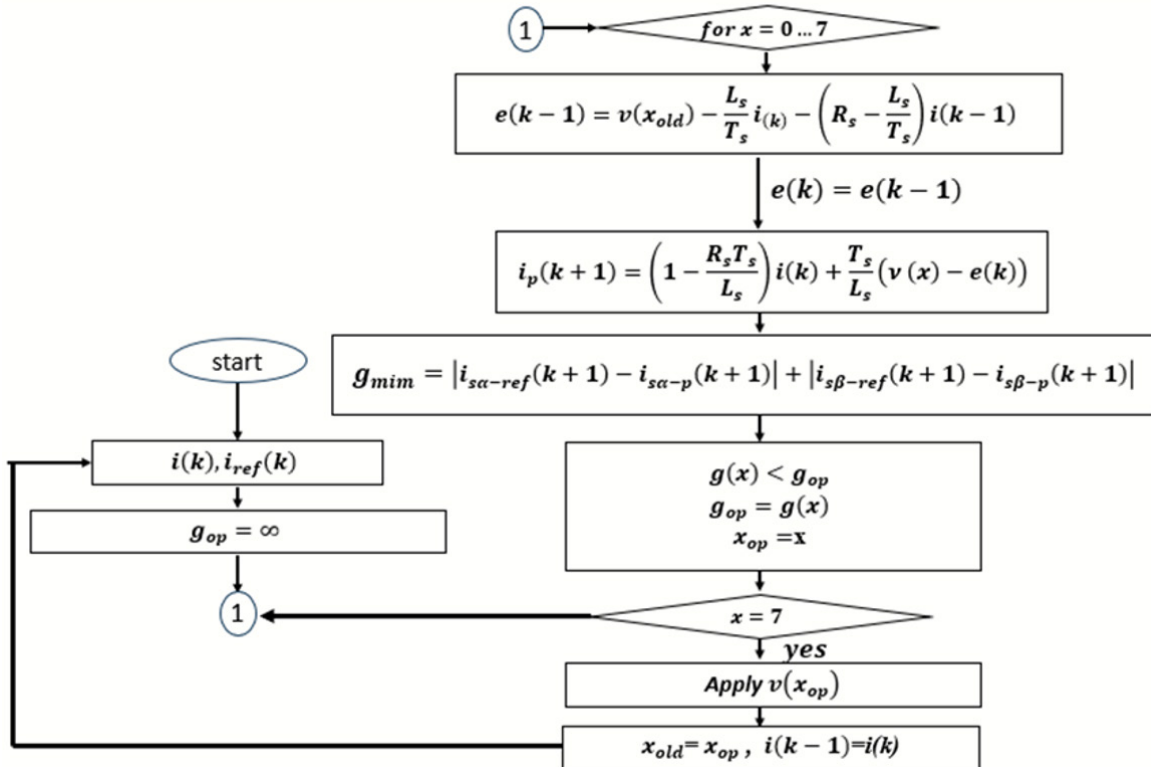


Figure 7. Flowchart of the PCC algorithm during each T_s .

As we can see, Figure 7 presents a detailed flowchart of the Predictive Current Control (PCC) algorithm, illustrating its operation during each sampling period T_s . This advanced control technique begins by measuring the current stator currents $i(k)$ and voltages $v(k)$ at the Machine Side Converter (MSC) terminals. The algorithm then estimates the back electromotive force (EMF) of the Permanent Magnet Synchronous Generator (PMSG). Using this information and the discrete model of the PMSG, the system predicts the future stator currents $i_p(k+1)$ for all possible voltage vectors that can be applied by the MSC. These predictions are then evaluated against the reference currents using a predefined cost function. The voltage vector that minimizes this cost function, i.e., produces the predicted current closest to the reference, is selected as the optimal control action. This chosen voltage vector is then applied to the MSC for the next sampling period. The process repeats continuously, allowing for rapid and precise current control without the need for a separate modulation stage. This method can potentially offer a faster dynamic response and more accurate current tracking compared to traditional PI-based control systems, potentially improving the overall efficiency and performance of the wind energy conversion system.

3.3. MPPT system

In the first stage of this research, the perturbation and observation (P&O) algorithm was used to estimate the optimal speed. Figure 8 presents the flowchart of the Perturbation and Observation (P&O) algorithm, a widely used method for Maximum Power Point Tracking (MPPT) in wind energy systems.

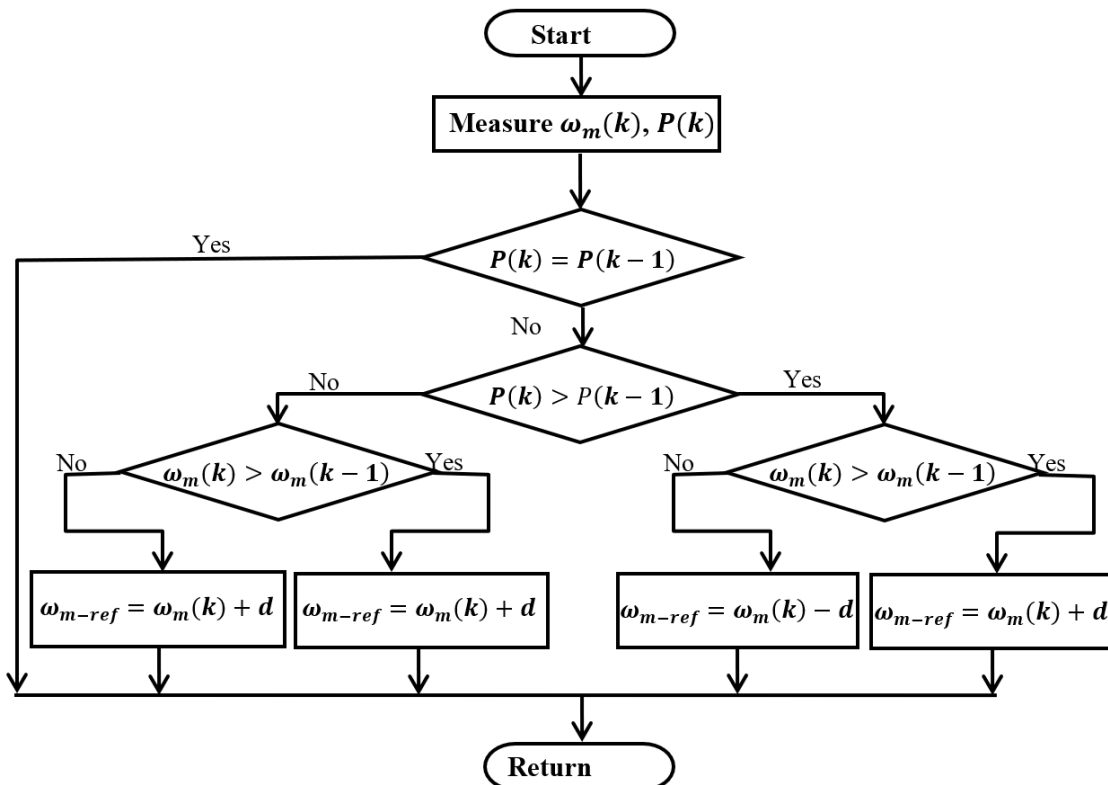


Figure 8. Flowchart of the P&O algorithm [7].

This iterative algorithm works by introducing small perturbations to the system's operating point and observing the resulting changes in power output. The process begins by measuring the current power $P(k)$ and comparing it to the previous power measurement $P(k-1)$. If an increase in power is observed, the algorithm continues to adjust the control variable (typically generator

speed or duty cycle) in the same direction. Conversely, if a decrease in power is detected, the algorithm reverses the direction of the perturbation. This simple yet effective approach allows the system to continuously seek and maintain operation at the maximum power point, adapting to changing wind conditions. However, it's worth noting that while the P&O method is easy to implement, it can result in oscillations around the maximum power point and may struggle with rapidly changing wind speeds.

In the second stage, it was relied on the TSR technique based on relationship 4. According to Figure 2, a TSR value must be maintained at 8.2, and thus the reference speed can be obtained as follows.

$$\omega_{m-ref} = \frac{8.2V}{R} \tag{17}$$

In the last stage, an artificial neural network was trained based on the results of operating the turbine generator model and extracting the current values corresponding to the rotation speed values that achieve maximum power at different wind speed values. Figure 9 illustrates the relationship between the generator's rotational speed and the corresponding optimal current values used to train an Artificial Neural Network (ANN) for Maximum Power Point Tracking (MPPT) in a wind energy conversion system. The graph shows a clear, non-linear correlation between these two parameters. As the rotational speed increases, the optimal current also increases, but not in a strictly linear fashion. This relationship is crucial for achieving maximum power extraction from the wind turbine across various wind speeds. The data points on this graph represent the results of operating the turbine-generator model at different wind speeds and extracting the current values that correspond to the rotational speeds achieving maximum power output. By training an ANN with this data, the control system can estimate the optimal current reference for any given rotational speed, eliminating the need for direct wind speed measurement. This approach combines the advantages of both Tip Speed Ratio (TSR) and Optimal Torque Control (OTC) techniques, potentially offering improved efficiency and adaptability. The use of an ANN for this purpose demonstrates an advanced, data-driven approach to MPPT, which can potentially outperform traditional methods in terms of speed, accuracy, and overall system efficiency.

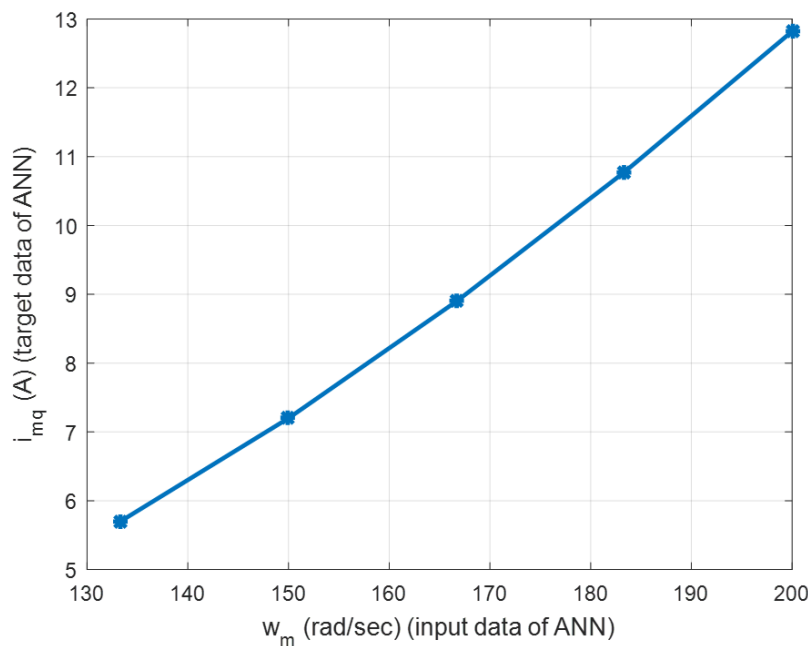


Figure 9. Current values according to speed.

Figure 10 illustrates an advanced control system for a Permanent Magnet Synchronous Generator (PMSG) in a wind energy conversion system. It combines a neural network-based Maximum Power Point Tracking (MPPT) system with a Predictive Current Control (PCC) system. The neural network uses the measured rotational speed to determine the optimal current reference values, which are then fed into the PCC system. This integration allows for efficient and dynamic control of the PMSG, potentially improving the overall performance and energy capture of the wind turbine system.

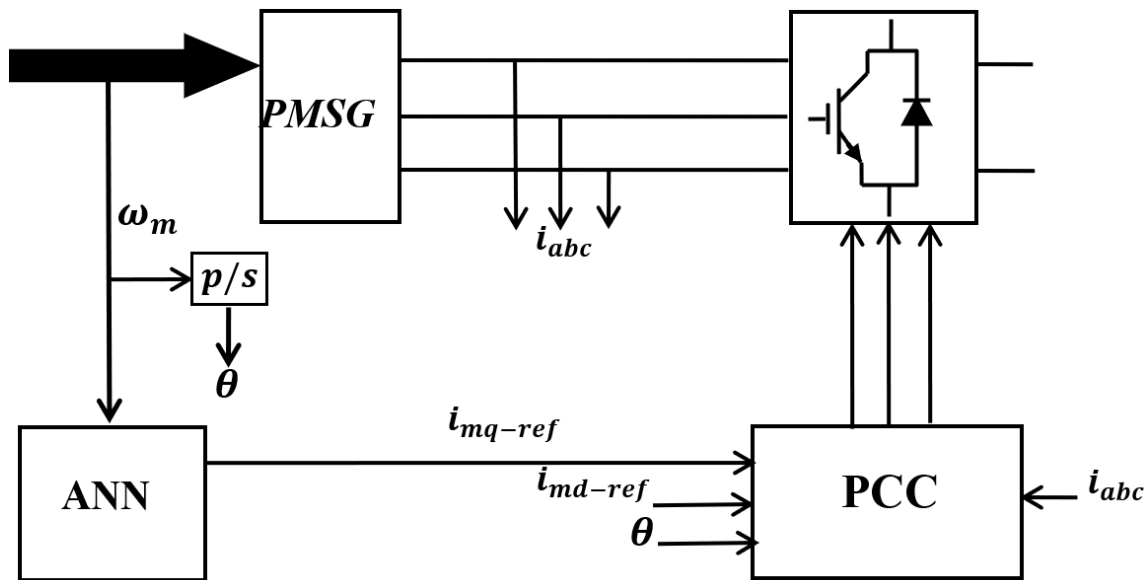


Figure 10. PMSG controls system using neural MPPT network and PCC system.

4. RESULTS AND DISCUSSION

Simulation was conducted in a Matlab/Simulink environment to test the performance of the proposed MPPT system and provide a comparison with other MPPT systems. Table 1 shows the parameter values of the generator used and the nominal values of voltage, current and speed.

Table1 Parameter values of the generator used and the nominal values.

Parameter	Value
R_{sm} , Stator resistance (Ω)	1.6
L_{mds} , inductances stator on d-axis (H)	6×10^{-3}
L_{mq_s} , inductances stator on q-axis (H)	6×10^{-3}
Φ_m , permanent magnet flux (Wb)	0.197
p , number of poles pairs	8
J , inertia torque (Kg.m^2)	1×10^{-3}
F , frictional constant (N.m.rad.sec^{-1})	1×10^{-5}
V_{phs} , Stator phase voltage (V)	225
I_{phs} , stator phase current (A)	9
ω_m , Mechanical speed (rad.sec^{-1})	200

Figure 11 depicts the simulated wind speed profile used to test the performance of the wind energy conversion system. The graph shows a step-wise increase in wind speed over time, starting

from an initial value of 8 m/s. The wind speed increases by 1 m/s every 0.5 seconds, creating a series of distinct steps. This controlled, incremental change in wind speed allows for a systematic evaluation of the system's response to varying wind conditions. By using such a structured wind profile, researchers can assess how quickly and accurately the control system adapts to changes in wind speed, particularly in terms of maximum power point tracking and overall system efficiency. This type of simulation is crucial for validating the performance of different control strategies under dynamic wind conditions before real-world implementation.

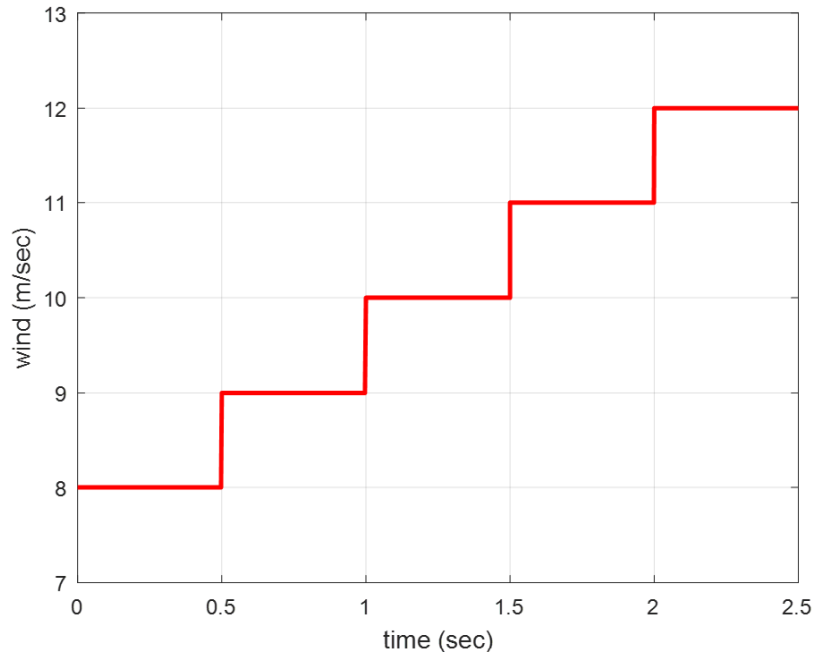


Figure 11. The assumed wind speed.

Figure 12 shows a comparative analysis of the rotational speed response for three different control systems in a wind energy conversion system.

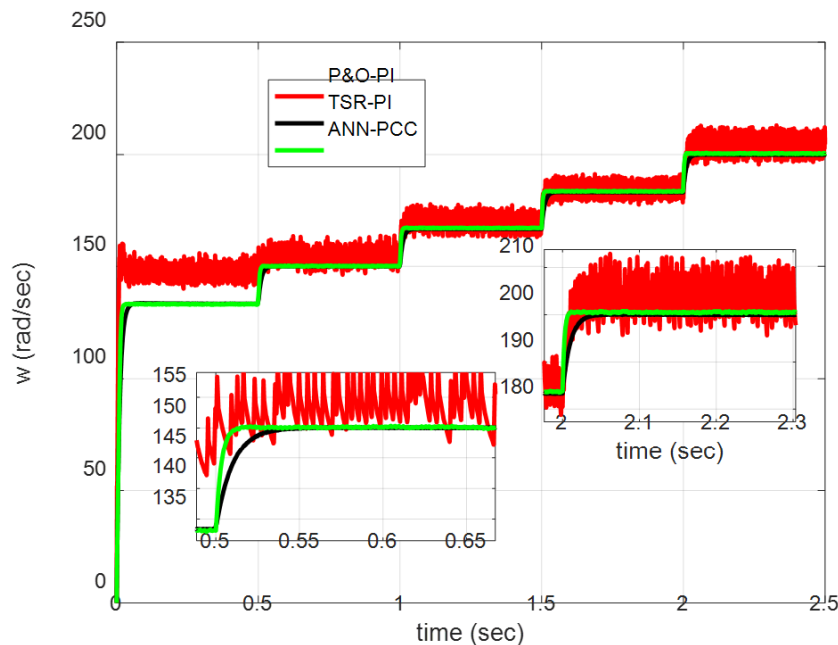


Figure 12. Rotational speed response for each of the three systems.

The graph shows how each control system - the proposed ANN-PCC (Artificial Neural Network with Predictive Current Control), TSR-PI (Tip Speed Ratio with Proportional-Integral control), and P&O-PI (Perturbation and Observation with PI control) - responds to the stepwise increases in wind speed depicted in Figure 11. The proposed ANN-PCC system demonstrates superior performance, characterized by rapid response times and minimal oscillations when adjusting to new wind speeds. It achieves steady-state in approximately 0.02 seconds, significantly outperforming the TSR-PI system, which takes about 0.06 seconds to stabilize. The P&O-PI system, while showing quick initial responses, exhibits considerable oscillations around the optimal speed value. These oscillations are a known limitation of the P&O algorithm, particularly in rapidly changing conditions. The graph clearly illustrates the advantages of the proposed ANN-PCC system in terms of speed, stability, and accuracy in tracking the optimal rotational speed for maximum power extraction. This improved performance could translate to higher overall system efficiency and better utilization of available wind energy across varying wind conditions.

Figure 13 illustrates the response of the generator current i_{md} (d-axis current) for each of the three control systems: ANN-PCC, TSR-PI, and P&O-PI. The graph demonstrates how effectively each system maintains the i_{md} current at its desired value of zero, which is crucial for optimal control of a surface-mounted Permanent Magnet Synchronous Generator (PMSG). The ANN-PCC and TSR-PI systems both show excellent performance in this regard, consistently maintaining the i_{md} current very close to zero with minimal fluctuations. This indicates that these control strategies are effective in decoupling the d-axis and q-axis controls, allowing for independent control of torque and flux. In contrast, the P&O-PI control system exhibits significant oscillations in the i_{md} current. These oscillations are a result of the inherent characteristics of the P&O algorithm, which continuously perturbs the system to find the maximum power point. While this approach can be effective for MPPT, it appears to introduce instability in the current control. The superior performance of the ANN-PCC and TSR-PI systems in maintaining a stable i_{md} current suggests that these control strategies may offer better overall system stability and efficiency, potentially leading to improved power quality and reduced mechanical stress on the generator.

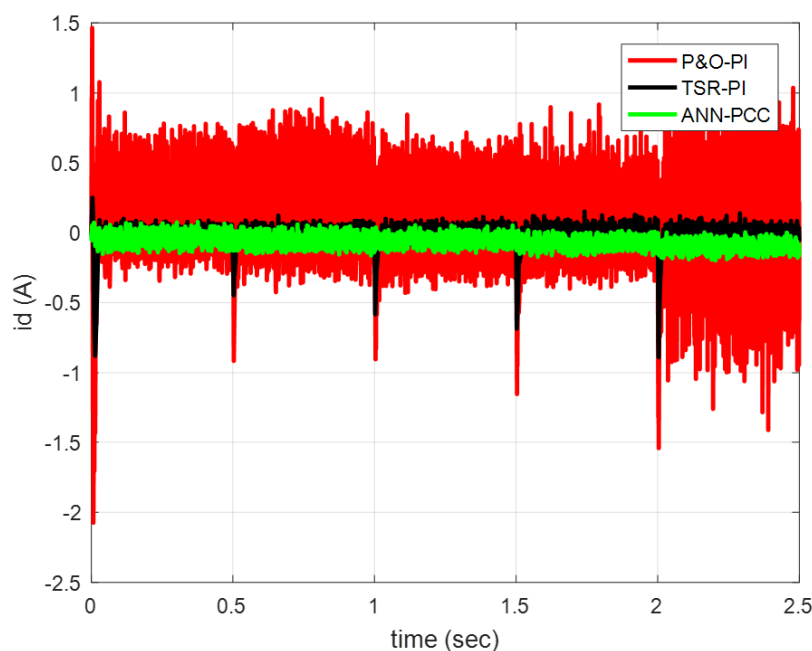


Figure 13. The generator current i_{md} for each of the three systems.

Figure 14 displays the amplitude of the PMSG phase current for each of the three control

systems: ANN-PCC, TSR-PI, and P&O-PI. The graph shows how the current amplitude changes in response to increasing wind speeds. Both the ANN-PCC and TSR-PI systems demonstrate smooth and stable current profiles, with the current increasing steadily as the wind speed rises. These systems effectively track the optimal current for maximum power extraction, reaching the nominal current of 9A at the generator's nominal speed. In contrast, the P&O-PI system exhibits significant oscillations in the current amplitude. This behavior is consistent with the inherent characteristics of the P&O algorithm, which continuously perturbs the system to find the maximum power point. The smooth current profiles of the ANN-PCC and TSR-PI systems suggest better power quality and potentially reduced mechanical stress on the generator compared to the P&O-PI system.

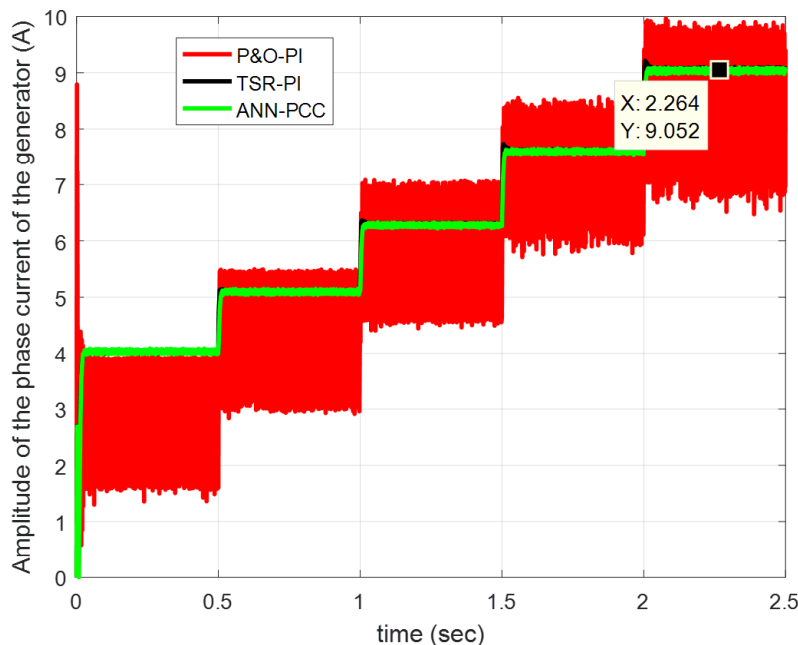


Figure 14. Amplitude of PMSG phases current for each of the three systems.

Figure 15 presents a comparative analysis of the PMSG phase voltage amplitude for three different control systems: ANN-PCC (Artificial Neural Network with Predictive Current Control), TSR-PI (Tip Speed Ratio with Proportional-Integral control), and P&O-PI (Perturbation and Observation with PI control). The graph illustrates how each system manages the generator voltage as wind speed increases over time. Both the ANN-PCC and TSR-PI systems demonstrate remarkably similar performance, characterized by smooth and stable voltage profiles. These systems show a steady increase in voltage amplitude as wind speed rises, effectively maintaining the optimal voltage for maximum power extraction. At the generator's nominal speed, both systems accurately reach and maintain the nominal voltage of 225V, indicating precise control and optimal energy conversion. In contrast, the P&O-PI system exhibits noticeable oscillations in the voltage amplitude. While it generally follows the upward trend with increasing wind speed, the fluctuations are significant and persistent. This behavior is consistent with the inherent characteristics of the P&O algorithm, which continuously perturbs the system to find the maximum power point. The smooth voltage profiles of the ANN-PCC and TSR-PI systems suggest better power quality, potentially reduced electrical stress on the generator, and more stable grid integration compared to the P&O-PI system. This comparison highlights the advantages of more advanced control strategies in maintaining stable and optimal generator voltage under varying wind conditions.

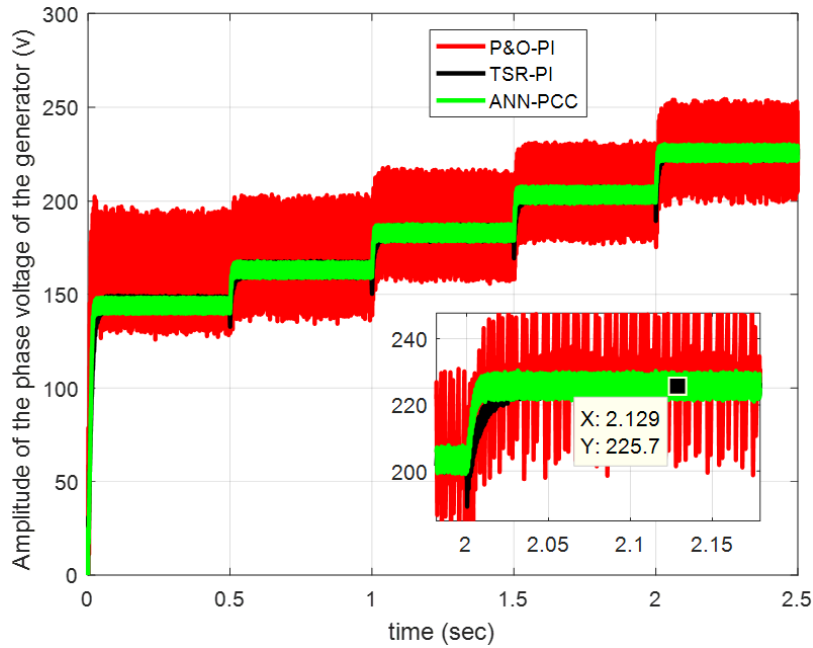


Figure 15. Amplitude of PMSG phases voltage for each of the three systems.

Figure 16 presents a comparison of the power output from the generator for each of the three control systems: ANN-PCC, TSR-PI, and P&O-PI. The figure demonstrates the performance of each system in tracking the maximum power point as wind speed increases. The ANN-PCC system shows superior performance, characterized by rapid response to wind speed changes and smooth power transitions.

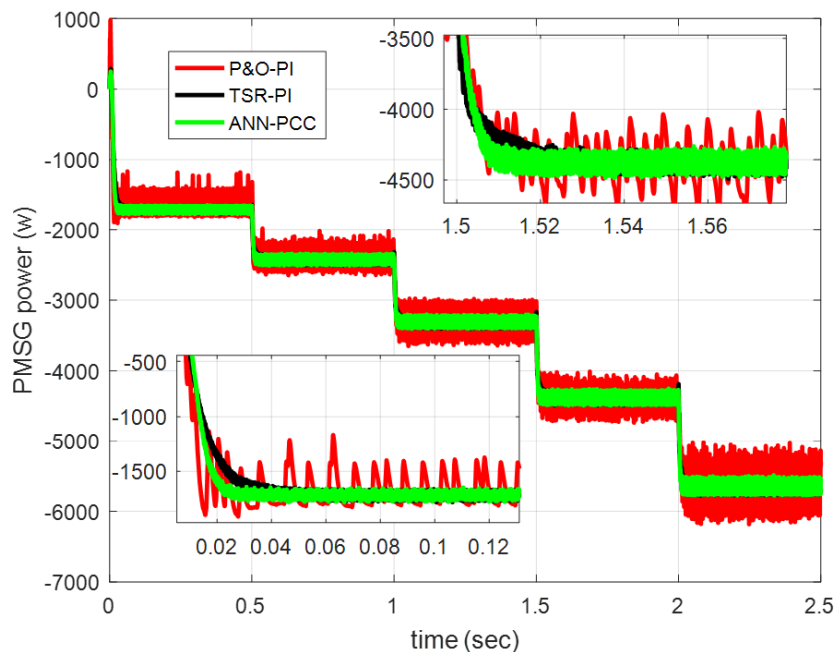


Figure 16. Power offered by the generator for each of the three systems.

It achieves the fastest tracking of the maximum power point, indicating excellent efficiency in energy extraction. The TSR-PI system also performs well, with smooth power curves, but exhibits slightly slower responses to wind speed changes compared to the ANN-PCC system. In contrast, the P&O-PI system, while showing quick initial responses to wind speed changes, suffers from significant power oscillations. These oscillations are a characteristic drawback of

the P&O algorithm, particularly in rapidly changing conditions. The graph effectively illustrates the trade-offs between speed of response and stability for each control method. The ANN-PCC system's ability to combine rapid response with smooth power output suggests it could provide significant advantages in real-world applications, potentially leading to higher overall energy yield and reduced mechanical stress on the turbine components. This comparison underscores the potential benefits of advanced control techniques like ANN-PCC in maximizing the efficiency of wind energy conversion systems.

Figure 17 illustrates the reactive power response for the three control systems: ANN-PCC, TSR-PI, and P&O-PI, in the wind energy conversion system. This graph is crucial in assessing the grid-side converter's performance in maintaining unity power factor operation. All three systems demonstrate the ability to regulate the reactive power close to zero, which is the desired outcome for optimal grid integration. The ANN-PCC and TSR-PI systems show particularly stable performance, with minimal fluctuations in reactive power across the entire simulation period. This indicates their effectiveness in decoupling active and reactive power control, ensuring that the system operates at unity power factor regardless of changes in wind speed or active power output. The P&O-PI system, while also maintaining near-zero reactive power on average, exhibits more noticeable oscillations. These fluctuations are consistent with the P&O algorithm's inherent characteristics of continuous system perturbation. The superior stability of the ANN-PCC and TSR-PI systems in reactive power control suggests better overall grid compatibility, potentially reducing stress on grid infrastructure and improving power quality. This comparison underscores the importance of advanced control strategies in optimizing the grid integration of wind energy systems.

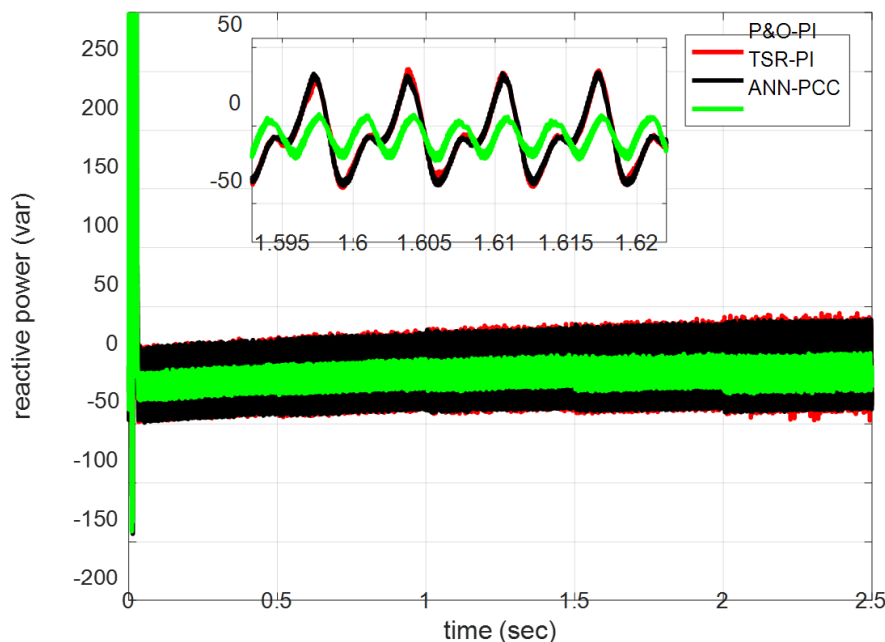


Figure 17. Reactive power for using the three control systems.

Figure 18 presents the DC link voltage regulation response for the three control systems: ANN-PCC, TSR-PI, and P&O-PI. This graph is crucial for assessing the stability and performance of the grid-side converter. Both the ANN-PCC and TSR-PI systems demonstrate excellent voltage regulation, maintaining a constant DC link voltage throughout the simulation period. This stability is maintained despite changes in wind speed and power output, indicating robust control performance. In contrast, the P&O-PI system shows noticeable fluctuations in the DC link voltage. While it generally maintains the voltage around the desired level, the oscillations are

significant and persistent. These fluctuations are consistent with the P&O algorithm's continuous perturbation approach. The superior performance of the ANN-PCC and TSR-PI systems in maintaining a stable DC link voltage suggests better overall system stability, potentially leading to improved power quality and more reliable grid integration.

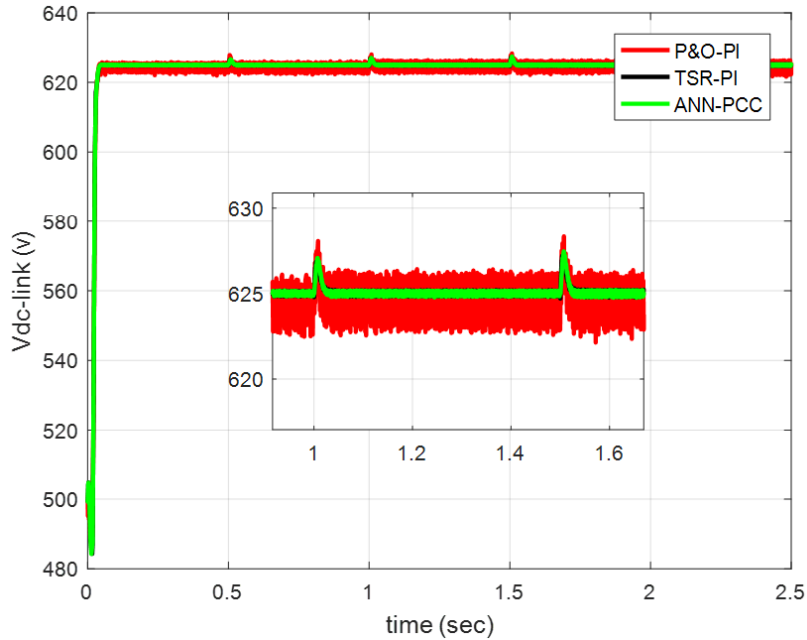


Figure 18. DC link voltage regulation response for using the three control systems.

Figure 19 illustrates the first phase current of the grid for each of the three control systems: ANN-PCC, TSR-PI, and P&O-PI. This graph provides crucial insights into the quality of power being injected into the grid by the wind energy conversion system under different control strategies. The ANN-PCC and TSR-PI systems demonstrate remarkably similar performance, characterized by smooth, near-sinusoidal current waveforms.

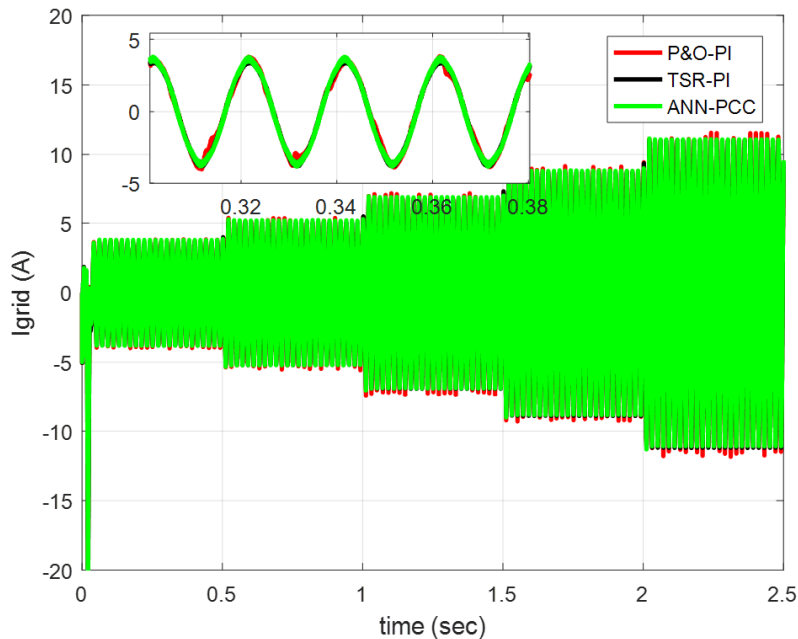


Figure 19. The first phase current of the grid when using the three control systems.

These waveforms maintain their quality consistently across the entire simulation period, even

as the wind speed and power output increase. The amplitude of the current grows steadily with increasing wind speed, reflecting the higher power output, but the waveform remains clean and stable. This indicates excellent harmonic control and suggests that these systems are likely to meet or exceed grid code requirements for power quality. In contrast, the P&O-PI system shows noticeable distortions in the current waveform. While the overall sinusoidal shape is maintained, there are visible ripples and irregularities superimposed on the main waveform. These distortions are consistent with the oscillatory nature of the P&O algorithm and its impact on both the DC link voltage and the generator currents. The presence of these distortions suggests that the P&O-PI system may have higher harmonic content in its output, potentially leading to power quality issues and possibly requiring additional filtering for grid compliance. The superior waveform quality demonstrated by the ANN-PCC and TSR-PI systems underscores their potential advantages in terms of grid integration, power quality, and overall system efficiency.

Figure 20 presents a comparative analysis of the Total Harmonic Distortion (THD) coefficient for the grid currents produced by the three control systems: ANN-PCC, TSR-PI, and P&O-PI. This graph is crucial for assessing the power quality of the wind energy conversion system and its compatibility with grid standards. The THD coefficient is plotted against time, allowing us to observe how it changes as the wind speed and power output increase throughout the simulation. The ANN-PCC system demonstrates the best performance, maintaining the lowest THD values consistently across the entire simulation period. This indicates superior harmonic control and suggests that this system would likely produce the cleanest power output, potentially exceeding grid code requirements for power quality.

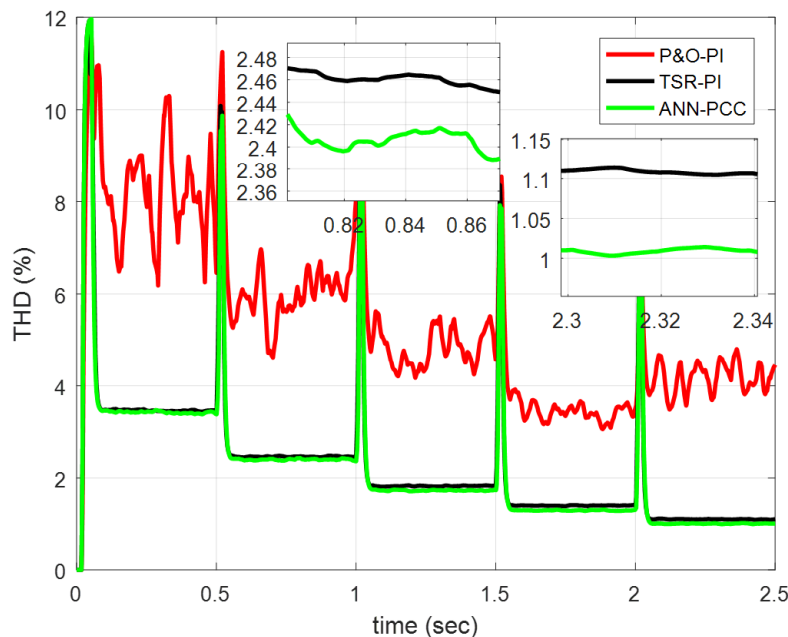


Figure 20. THD coefficient changes when using the three control systems.

The TSR-PI system also performs well, showing slightly higher but still very low THD values compared to the ANN-PCC system. Both these systems maintain THD levels well below typical grid standards, which often require THD to be less than 5%. In stark contrast, the P&O-PI system exhibits significantly higher THD values throughout the simulation. The THD for this system not only starts at a higher level but also shows more fluctuation and a general increasing trend as the simulation progresses. This poor THD performance is consistent with the visible current waveform distortions observed in Figure 19 for the P&O-PI system. The high THD values suggest that this system would likely require additional filtering or power conditioning to meet grid code

requirements, potentially increasing system complexity and cost. The superior THD performance of the ANN-PCC and TSR-PI systems underscores their potential advantages in terms of grid integration and overall system efficiency. Lower THD values translate to reduced stress on grid infrastructure, lower losses, and potentially simpler and less costly grid connection equipment. This comparison demonstrates the importance of advanced control strategies in optimizing the power quality of wind energy conversion systems.

The system effectively handles stepwise increases in wind speed by rapidly adjusting the generator's rotational speed without significant overshooting or instability, as shown in the simulation results with wind speed changes of 1 m/s every 0.5 seconds. The neural network's ability to estimate optimal reference currents based solely on rotational speed measurements allows the system to quickly adapt to changing conditions without requiring direct wind speed measurements, while the predictive current control ensures precise current regulation throughout these transitions.

Table 2 Comparison between the proposed system and other control systems.

System	Tracking speed	THD coefficient of grid Current	Efficiency	The need for wind speed measurement
P&O-PI	High	High	low	No
TSR-PI	High	low	High	Yes
ANN-PCC	Very High	Very low	High	No

Table 2 provides a comprehensive comparison of the three control systems - P&O-PI, TSR-PI, and ANN-PCC - across four crucial performance metrics. The P&O-PI system shows high tracking speed but suffers from high THD in grid current, low efficiency, and doesn't require wind speed measurement. The TSR-PI system demonstrates high tracking speed, low THD, and high efficiency, but necessitates wind speed measurement. The system demonstrates exceptional grid-side performance through several key characteristics. It achieves near-perfect unity power factor operation by precisely controlling q-axis current to zero while maintaining remarkably stable DC link voltage even during wind speed variations. The control strategy produces high-quality sinusoidal current waveforms with minimal harmonic distortion, contributing to superior power quality at the grid interface. Additionally, the system effectively suppresses reactive power fluctuations through its advanced control algorithms, ensuring smooth and efficient power transfer to the grid with reduced stress on both the converter and grid infrastructure, ultimately leading to more reliable and efficient grid integration of wind energy.

The proposed ANN-PCC system excels in all categories, offering very high tracking speed, very low THD, and high efficiency, and eliminates the need for wind speed measurement. This comparison highlights the ANN-PCC system's superior performance, combining the advantages of both P&O and TSR methods while overcoming their respective limitations. The ANN-PCC's ability to achieve high efficiency and power quality without wind speed measurement represents a significant advancement in wind energy conversion system control.

The proposed system achieves significantly faster response times; reaching steady-state in approximately 0.02 seconds compared to 0.06 seconds for TSR-PI, while exhibiting minimal oscillations during wind speed changes. It maintains excellent stability in controlling the generator's d-axis current (i_{md}), keeping it consistently at zero with minimal fluctuations, unlike the P&O-PI system which shows considerable oscillations. The ANN-PCC approach also simplifies the overall system architecture by eliminating the need for wind speed sensors and separate speed regulation loops, while still maintaining maximum power point tracking capabilities. These improvements result in enhanced dynamic performance, higher overall efficiency, and better stability under variable wind conditions.

5. CONCLUSIONS

To sum up, this study introduces a novel approach to enhancing the efficiency and dynamic performance of PMSG-based wind energy conversion systems through the integration of Artificial Neural Networks (ANN) and Predictive Current Control (PCC). The proposed ANN-PCC control system demonstrates significant advantages over conventional control methods, including faster maximum power point tracking, improved stability under variable wind conditions, and reduced total harmonic distortion. By eliminating the need for wind speed measurement and the speed regulation loop, the system achieves a simpler architecture while maintaining high performance. Simulation results confirm the superiority of the ANN-PCC approach in terms of response time, power output stability, and grid current quality compared to traditional P&O-PI and TSR-PI control systems. These improvements contribute to the overall efficiency and reliability of wind power generation, potentially facilitating broader adoption of wind energy technology. Moreover, by eliminating the need for wind speed sensors and reducing system complexity while improving performance, the proposed system offers potential cost savings in both initial installation and long-term maintenance, making it an economically attractive solution for wind energy systems. Future work should focus on several key areas to further advance this research. Firstly, experimental validation of the proposed control system on a physical PMSG-based wind turbine would provide valuable insights into its real-world performance and practical implementation challenges. Secondly, investigating the system's behavior under extreme weather conditions and grid faults would enhance its robustness and reliability. Thirdly, exploring the integration of energy storage systems with the proposed control strategy could address intermittency issues inherent in wind power generation. Additionally, extending the ANN-PCC approach to other types of renewable energy systems, such as solar PV or hybrid wind-solar systems could yield interesting results. Finally, incorporating advanced machine learning techniques, such as reinforcement learning or adaptive neural networks, could potentially further improve the system's ability to optimize performance in real time under varying environmental and grid conditions.

Author Contributions: Conceptualization B. A., M. S., and M. B; methodology, B. A., M. S., M. B., R. R.I., and M. T; validation, B. A., M. S., and M. B; formal analysis, B. A., M. S., M. B., R. R.I., and M. T; resources, all authors; data Curation, all authors; writing—original draft preparation, all authors; writing—review and editing, B. A., M. S., M. B., R. R.I., and M. T; All authors have read and agreed to the published version of the manuscript.

Funding statement: This research received no external funding.

Data Availability Statement: Not applicable.

Conflicts of Interest: The authors declare that they have no conflict of interest.

Data Availability: The data are available at request.

Acknowledgements: This work was supported by the General Directorate of Scientific Research and Technological Development (DGRSDT), the body affiliated to the Algerian Ministry of Higher Education and Scientific Research.

REFERENCES

- [1] Dursun, E. H., Kulaksiz, A. A.: *Second-order sliding mode voltage-regulator for improving MPPT efficiency of PMSG-based WECS. International Journal of Electrical Power & Energy Systems.* 121, 106149 (2020). <https://doi.org/10.1016/j.ijepes.2020.106149>
- [2] Dali, A., Abdelmalek, S., Bakdi, A., Bettayeb, M.: *A new robust control scheme: Application for MPP tracking of a PMSG-based variable-speed wind turbine. Renewable Energy.* 172, 1021-1034 (2021). <https://doi.org/10.1016/j.renene.2021.03.083>

-
- [3] Abouddrar, I., El Hani, S., Heyine, M. S., Naseri, N.: *Dynamic Modeling and Robust Control by ADRC of Grid-Connected Hybrid PV-Wind Energy Conversion System*. *Mathematical Problems in Engineering*. 1, 8362921 (2019). <https://doi.org/10.1155/2019/8362921>
- [4] Fannakh, M., Elhafyani, M. L., Zouggar, S., Zahboune, H.: *Overall fuzzy logic control strategy of direct driven PMSG wind turbine connected to grid*. *Int. J. Electr. Comput. Eng. IJECE*. 11, 5515 (2021). <https://doi.org/10.11591/ijece.v11i6.pp5515-5529>
- [5] Youssef, A. R., Ali, A. I., Saeed, M. S., Mohamed, E. E.: *Advanced multi-sector P&O maximum power point tracking technique for wind energy conversion system*. *International Journal of Electrical Power & Energy Systems*. 107, 89-97 (2019). <https://doi.org/10.1016/j.ijepes.2018.10.034>
- [6] Sai Manoj, P., Vijayakumari, A., Kottayil, S. K.: *Development of a comprehensive MPPT for grid-connected wind turbine driven PMSG*. *Wind Energy*. 22(6), 732-744 (2019). <https://doi.org/10.1002/we.2318>
- [7] Meghni, B., Saadoun, A., Dib, D., Amirat, Y.: *Effective MPPT technique and robust power control of the PMSG wind turbine*. *IEEE Transactions on Electrical and Electronic Engineering*. 10(6), 619-627 (2015). <https://doi.org/10.1002/tee.22128>
- [8] ElMourabit, Y., Derouich, A., El Ghzizal, A., El Ouanjli, N., Zamzoum, O.: *Nonlinear back-stepping control for PMSG wind turbine used on the real wind profile of the Dakhla-Morocco city*. *International Transactions on Electrical Energy Systems*. 30(4), e12297 (2020). <https://doi.org/10.1002/2050-7038.12297>
- [9] Chen, J., Yao, W., Zhang, C. K., Ren, Y., Jiang, L.: *Design of robust MPPT controller for grid-connected PMSG-Based wind turbine via perturbation observation based nonlinear adaptive control*. *Renewable energy*. 134, 478-495 (2019). <https://doi.org/10.1016/j.renene.2018.11.048>
- [10] Errami, Y., Obbadi, A., Sahnoun, S., Benhmida, M., Ouassaid, M., Maaroufi, M.: *Design and sliding mode control for PMSG based wind power system connected to a non-ideal grid voltages*. In *2015 3rd International Renewable and Sustainable Energy Conference (IRSEC)* (pp.1-7).IEEE (2015). <https://doi.org/10.1109/IRSEC.2015.7454981>
- [11] Agarwal, N. K., Sadhu, P. K., Chakraborty, S.: *Mpmt based pmsg wind turbine system using sliding model control (SMC) and artificial neural network (ANN) based regression analysis*. *IETE Journal of research*. 68(3), (2022), 1652-1660. <https://doi.org/10.1080/03772063.2019.1662336>
- [12] Zafran, M., Khan, L., Khan, Q., Alam, Z., Khan, M. A.: *Terminal sliding mode based finite-time MPPT control for PMSG-WECS based standalone system*. In *2020 3rd International Conference on Computing, Mathematics and Engineering Technologies (iCoMET)* (pp. 1-7).IEEE (2020). <https://doi.org/10.1109/iCoMET48670.2020.9073906>
- [13] Babu, P. S., Sundarabalan, C. K., Balasundar, C., Krishnan, T. S.: *Fuzzy logic based optimal tip speed ratio MPPT controller for grid connected WECS*. *Materials Today: Proceedings*. 45, 2544-2550 (2021). <https://doi.org/10.1016/j.matpr.2020.11.259>
- [14] Yang, H., Wei, Z., Chengzhi, L.: *Optimal design and techno-economic analysis of a hybrid solar-wind power generation system*. *Applied energy*, 86(2), 163-169 (2009). <https://doi.org/10.1016/j.apenergy.2008.03.008>
- [15] Moutchou, R., Abbou, A.: *Control of grid side converter in wind power based PMSG with PLL method*. *International Journal of Power Electronics and Drive Systems (IJPEDS)*, 12(4) (2021), 2191-2200. <https://doi.org/10.11591/ijpeds.v12.i4.pp2191-2200>
- [16] Baran, J., Jqaderko, A.: *An MPPT control of a PMSG-based WECS with disturbance compensation and wind speed estimation*. *Energies*, 13(23), 6344 (2020). <https://doi.org/10.3390/en13236344>

- [17] Salem, A. A., Aldin, N. A. N., Azmy, A. M., Abdellatif, W. S.: *Implementation and validation of an adaptive fuzzy logic controller for MPPT of PMSG-based wind turbines.* IEEE Access, 9, 165690-165707 (2021). <https://doi.org/10.1109/ACCESS.2021.3134947>
- [18] Mahmoud, M. M., Aly, M. M., Salama, H. S., Abdel-Rahim, A. M. M.: *A combination of an OTC based MPPT and fuzzy logic current control for a wind-driven PMSG under variability of wind speed.* Energy Systems, 13(4) (2022), 1075-1098. <https://doi.org/10.1007/s12667-021-00468-2>
- [19] Barradi, Y., Zazi, K., Zazi, M., Khaldi, N.: *Control of PMSG based variable speed wind energy conversion system connected to the grid with PI and ADRC approach.* International Journal of Power Electronics and Drive Systems. 11(2), 953 (2020). <http://doi.org/10.11591/ijpeds.v11.i2.pp953-968>
- [20] Prince, M. K. K., Arif, M. T., Gargoom, A., Oo, A. M., Haque, M. E.: *Modeling, parameter measurement, and control of PMSG-based grid-connected wind energy conversion system.* Journal of Modern Power Systems and Clean Energy. 9(5), (2021)1054-1065. <https://doi.org/10.35833/MPCE.2020.000601>
- [21] Chandrasekaran, K., Mohanty, M., Golla, M., Venkadesan, A., Simon, S. P.: *Dynamic MPPT controller using cascade neural network for a wind power conversion system with energy management.* IETE Journal of Research, 68(5), (2022) 3316-3330. <https://doi.org/10.1080/03772063.2020.1756934>
- [22] Rachedi, M. O., Saidi, M. L., Arbaoui, F.: *MPPT control design for variable speed wind turbine.* International Journal of Electrical and Computer Engineering (IJECE), 10(5), (2020) 4604-4614. <https://doi.org/10.11591/ijece.v10i5.pp4604-4614>
- [23] Tahiri, F. E., Chikh, K., El Afia, A., Lamterkati, J., Khafallah, M.: *Simulation and experimental validation of VOC and hysteresis control strategies of unit power factor three-phase PWM rectifier.* In 2017 International Conference on Electrical and Information Technologies (ICEIT) (pp. 1-6). IEEE (2017). <https://doi.org/10.1109/EITech.2017.8255238>
- [24] Abouddrar, I., El Hani, S., Mediouni, H., Aghmad, A., Heyine, M. S.: *Robust control of three phase grid connected PV system based on ADRC and fuzzy.* In 2018 6th International Renewable and Sustainable Energy Conference (IRSEC) (pp. 1-6).IEEE (2018). <https://doi.org/10.1109/IRSEC.2018.8702950>
- [25] Devanshu, A., Singh, M., & Kumar, N.: *Adaptive predictive current control of field-oriented controlled induction motor drive.* IETE Journal of Research, 68(5), (2022) 3707-3719. <https://doi.org/10.1080/03772063.2020.1775502>
- [26] Zhang, Y., Xia, B., Yang, H., Rodriguez, J.: *Overview of model predictive control for induction motor drives.* Chinese Journal of Electrical Engineering, 2(1), 62-76 (2016). <https://doi.org/10.23919/CJEE.2016.7933116>